Supporting Information

Quantifying how the cis/trans ratio of N,N-dimethyl-3,5-dimethylpiperidinium hydroxide impacts the growth kinetics, composition and local structure of SSZ-39

Zheng Cui,[a] Charles E. Umhey,[b] Onyinyechukwu C. Ukagha,[a] Motunrayo Ogunleye,[a] Jean-Sabin McEwen,[b,c,d,e,f] and Daniel F. Shantz[a,*]

[a]Department of Chemical and Biomolecular Engineering, 6823 St. Charles Avenue, New Orleans, LA 70118, United States. Email: dshantz@tulane.edu
[b]The Gene and Linda Voiland School of Chemical Engineering and Bioengineering, Washington State University, Pullman, WA 99164, United States
[c]Institute for Integrated Catalysis, Pacific Northwest National Laboratory, Richland, WA 99352, United States
[d]Department of Physics and Astronomy, Washington State University, Pullman, WA 99164, United States
[e]Department of Chemistry, Washington State University, Pullman, WA 99164, United States
[f]Department of Biological Systems Engineering, Washington State University, Pullman, WA 99164, United States

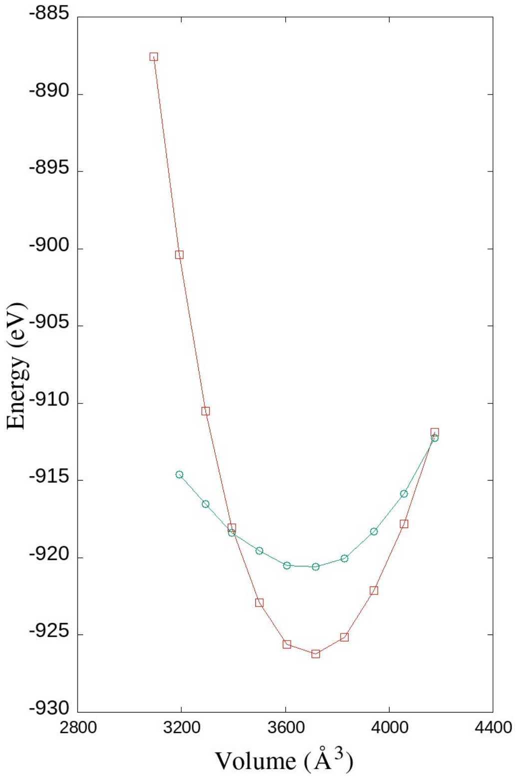

Figure S1. Energy Volume Plot for FAU using the optB86b-vdW functional (red squares) and optB88B-vdw functional (green circles).

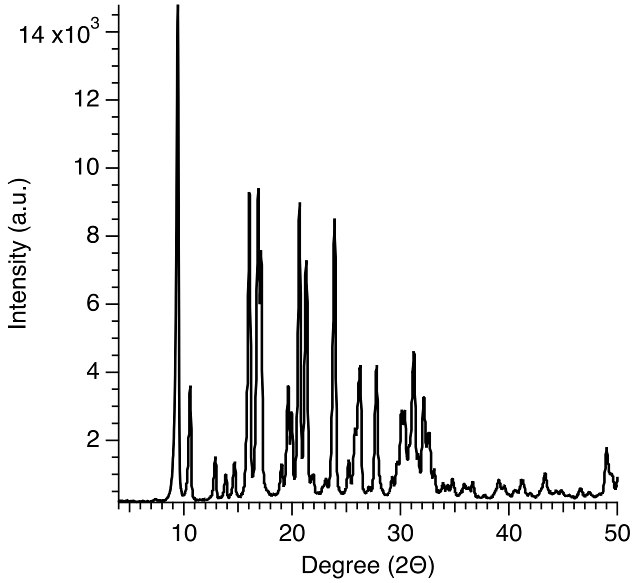

Figure S2. PXRD of SSZ-39.

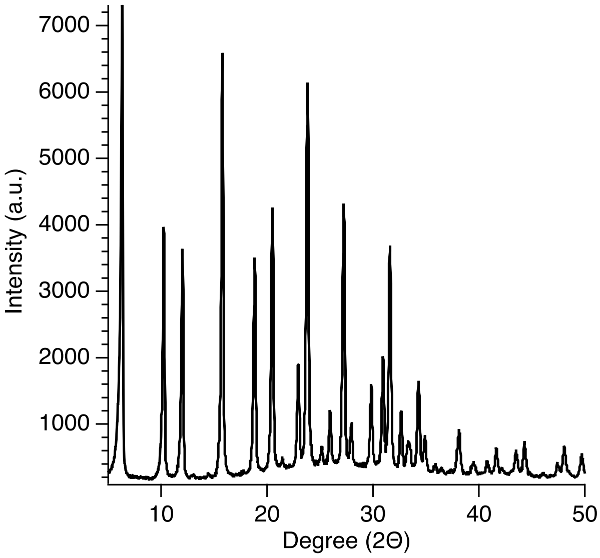

Figure S3. PXRD of parent FAU.

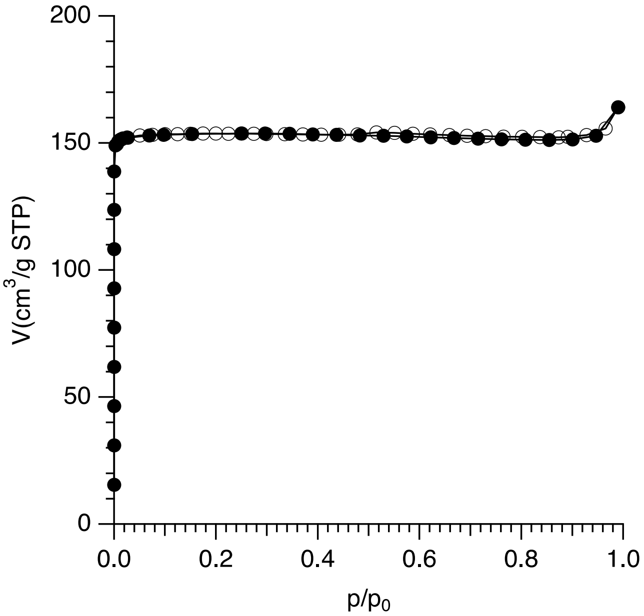

Figure S4. Nitrogen adsorption isotherm of SSZ-39.

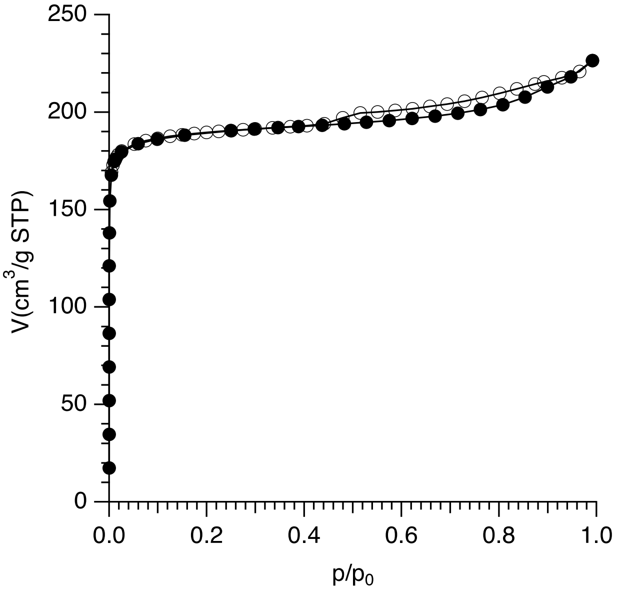

Figure S5. Nitrogen adsorption isotherm of parent FAU.

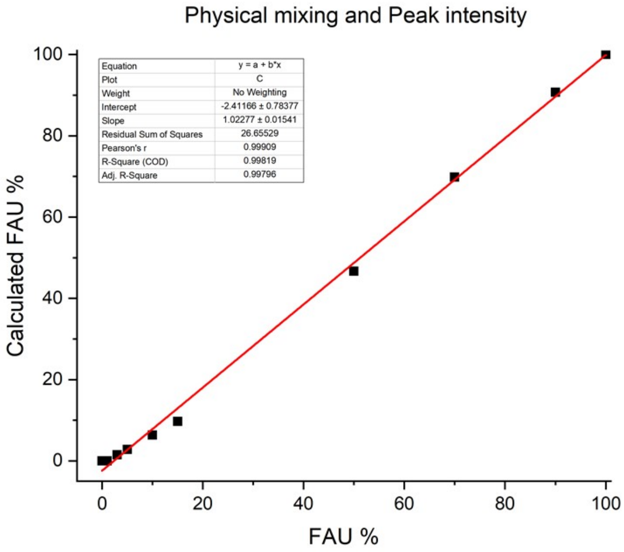

Equation	y = a + b*x
Plot	C
Weight	No Weighting
Intercept	-2.41166 ± 0.78377
Slope	1.02277 ± 0.01541
Residual Sum of Squares	26.65529
Pearson's r	0.99909
R-Square (COD)	0.99819
Adj. R-Square	0.99796

Figure S6. Physical mixing and Peak intensity of known quantities of FAU and SSZ-39.

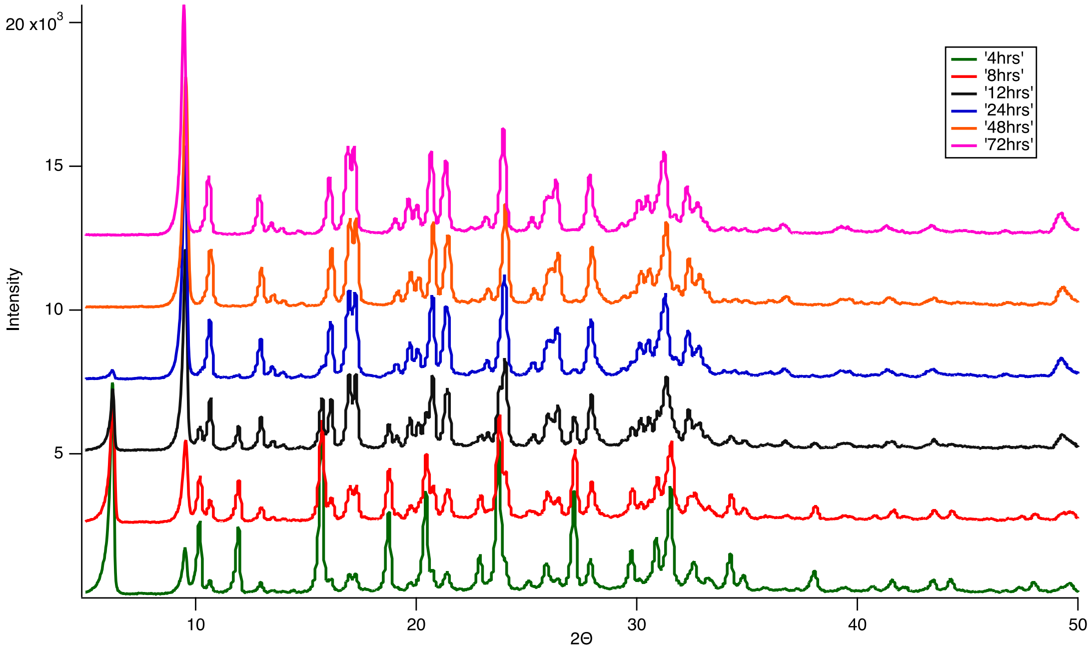

Figure S7. PXRD of calcined samples made with 14% trans OSDA made at different synthesis times.

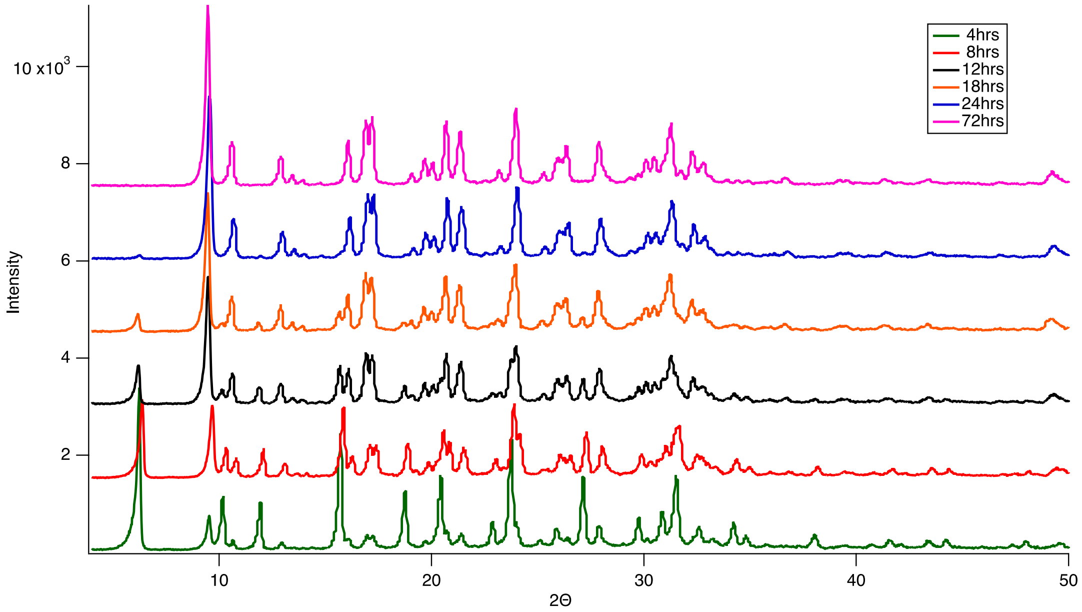

Figure S8. PXRD of calcined samples made with 26% trans OSDA made at different synthesis times.

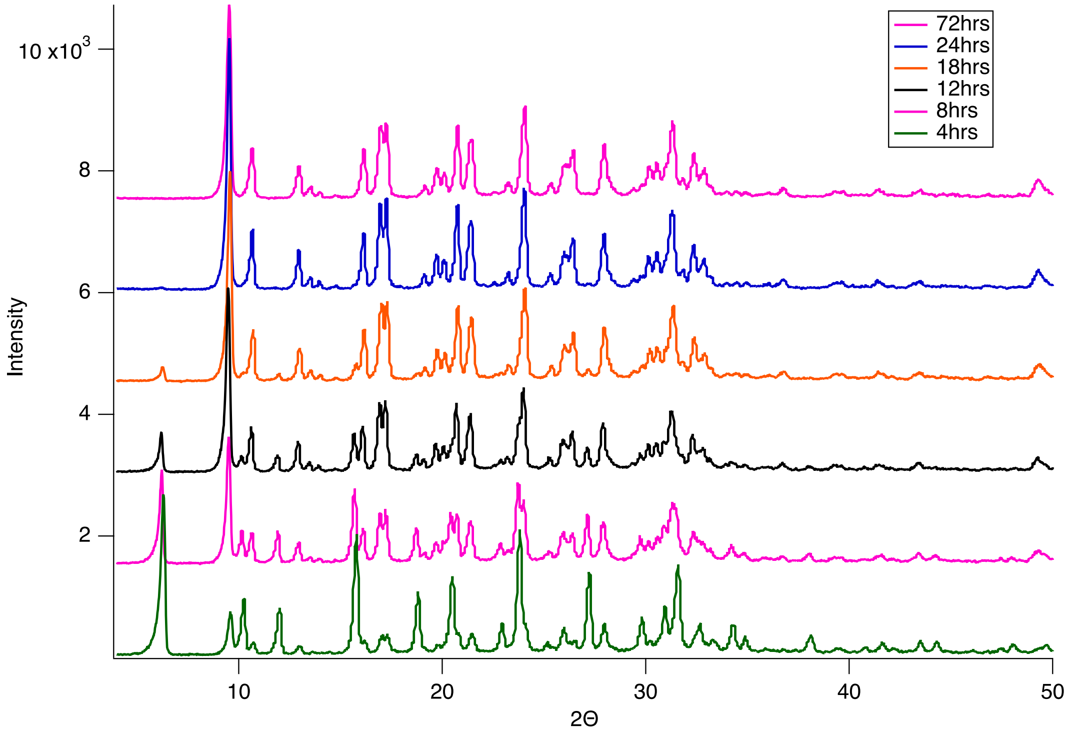

Figure S9. PXRD of calcined samples made with 54% trans OSDA made at different synthesis times.

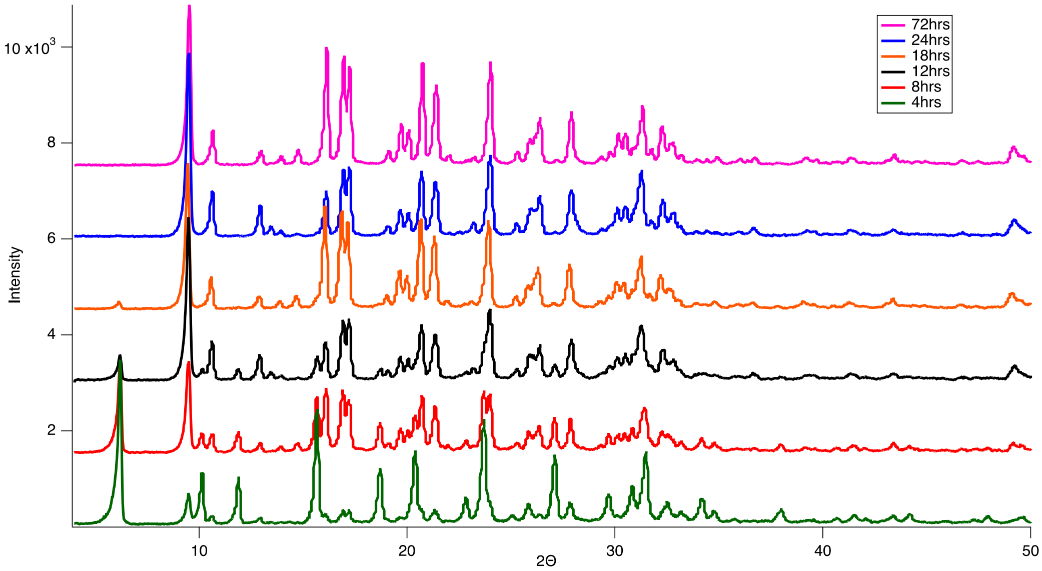

Figure S10. PXRD of calcined samples made with 80% trans OSDA made at different synthesis times.

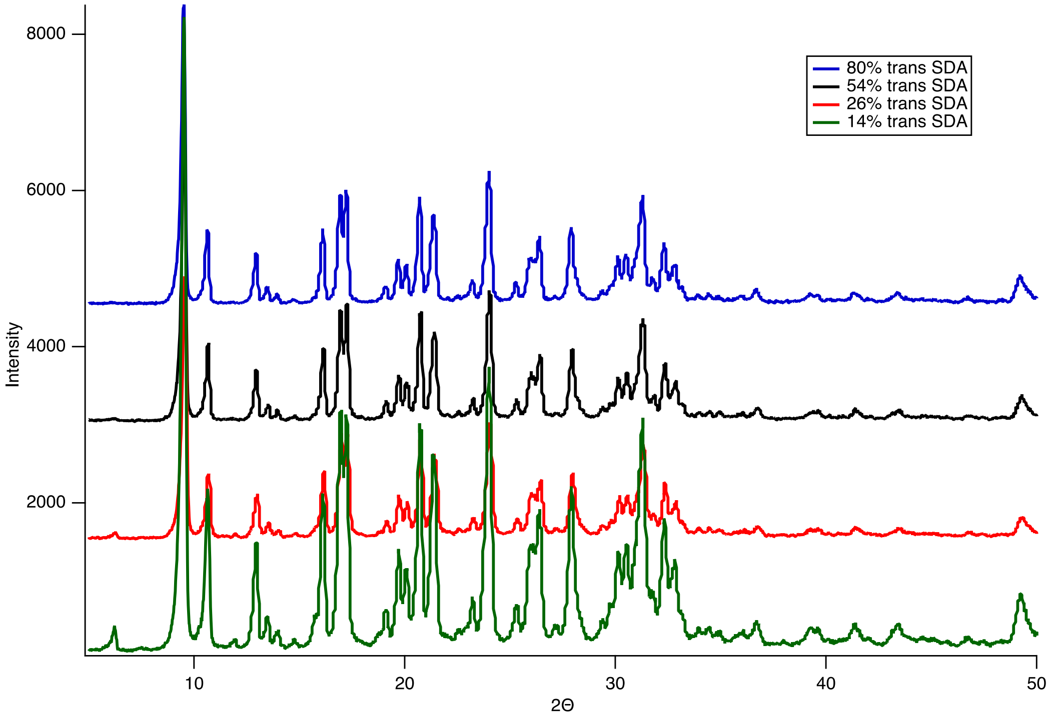

Figure S11. PXRD of calcined samples made with different OSDA content after 24 hours of heating.

FAU

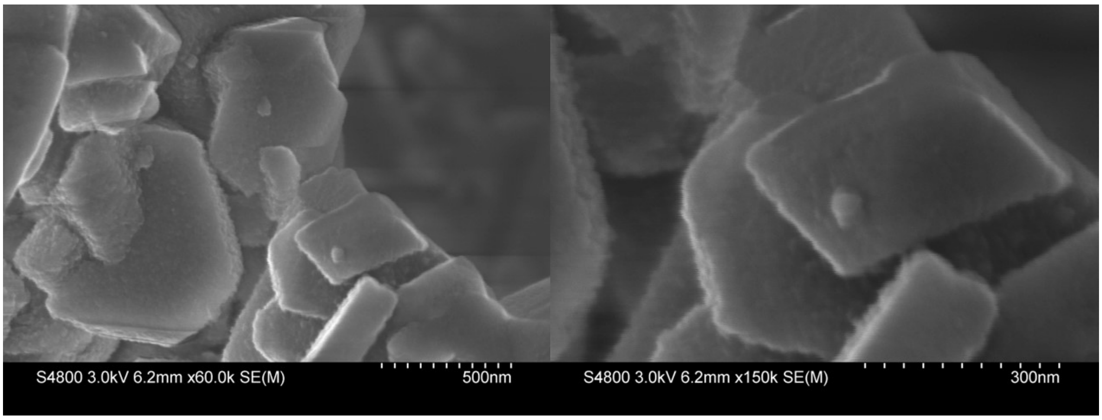
S4800 3.0kV 6.2mm x60.0k SE(M) 500nm
S4800 3.0kV 6.2mm x150k SE(M) 300nm

2h

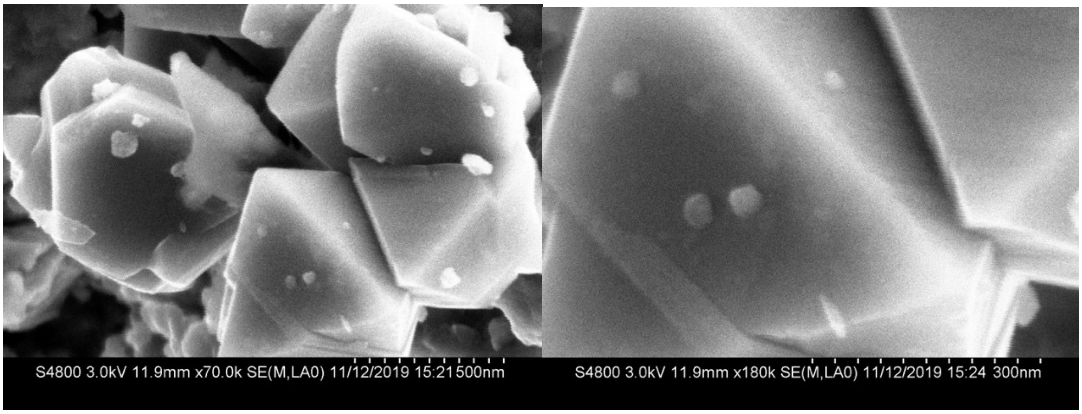
S4800 3.0kV 11.9mm x70.0k SE(M,LA0) 11/12/2019 15:21 500nm
S4800 3.0kV 11.9mm x180k SE(M,LA0) 11/12/2019 15:24 300nm

3h

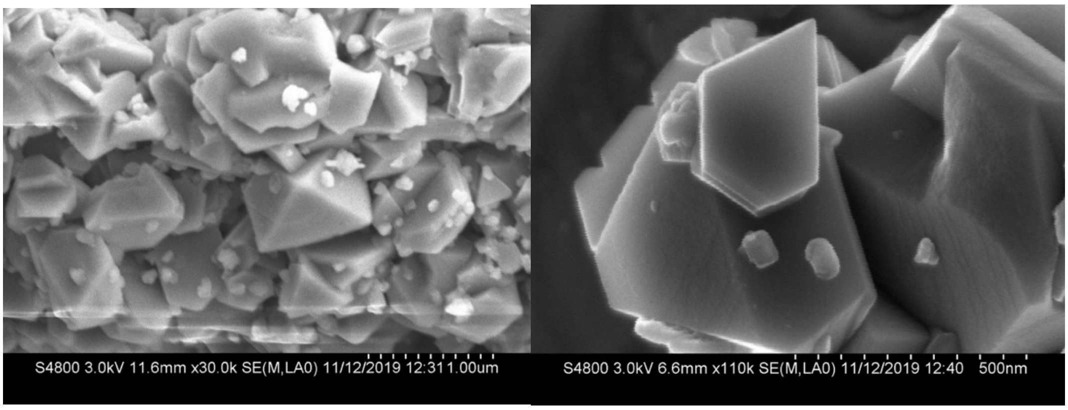
S4800 3.0kV 11.6mm x30.0k SE(M,LA0) 11/12/2019 12:31 1.00um
S4800 3.0kV 6.6mm x110k SE(M,LA0) 11/12/2019 12:40 500nm

4h

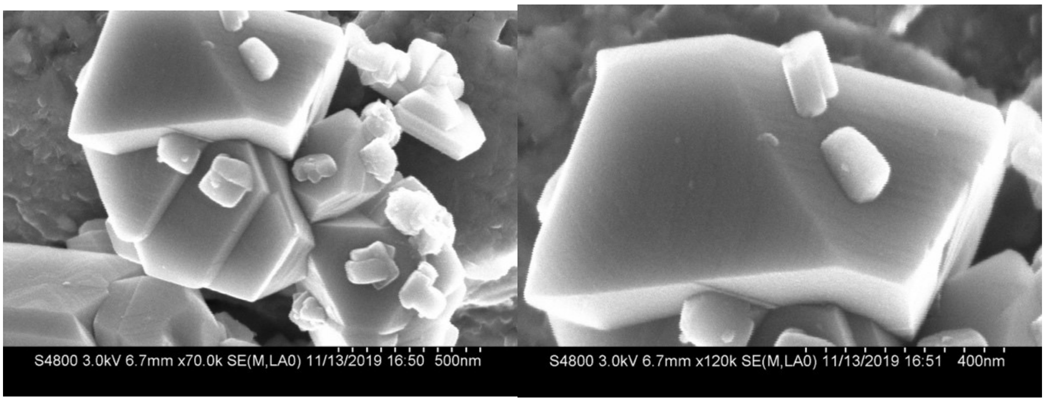
S4800 3.0kV 6.7mm x70.0k SE(M,LA0) 11/13/2019 16:50 500nm
S4800 3.0kV 6.7mm x120k SE(M,LA0) 11/13/2019 16:51 400nm

8h

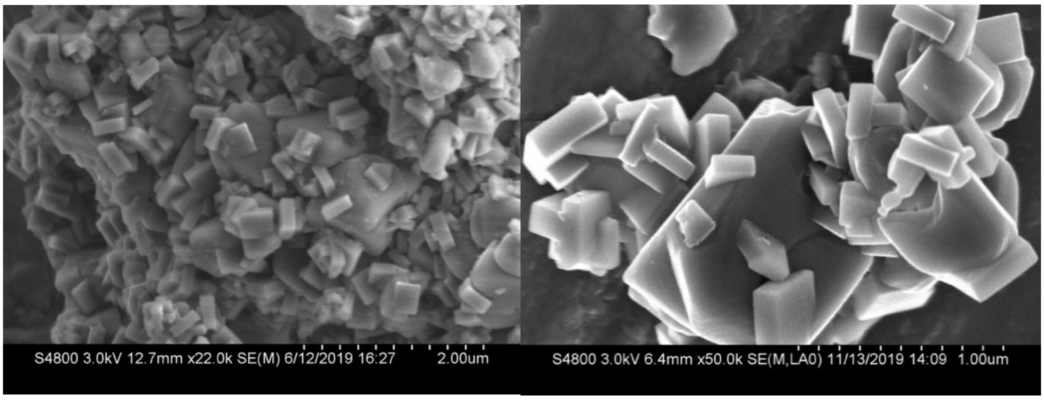

12h

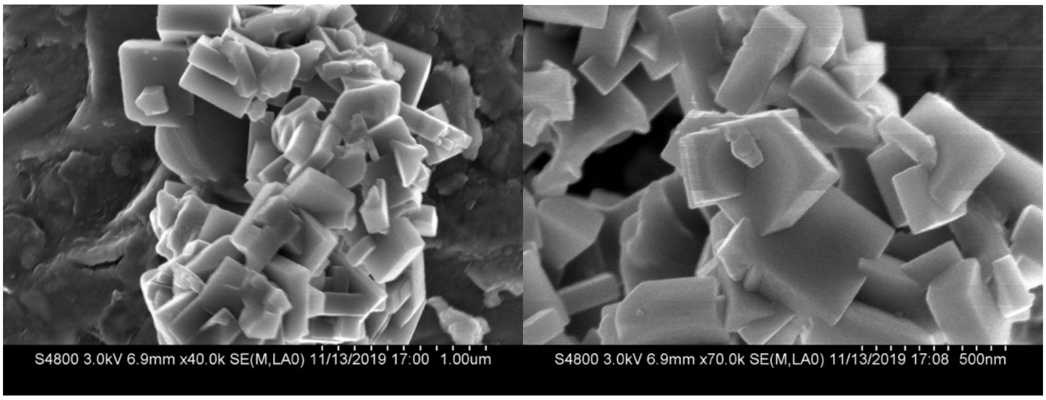

24h

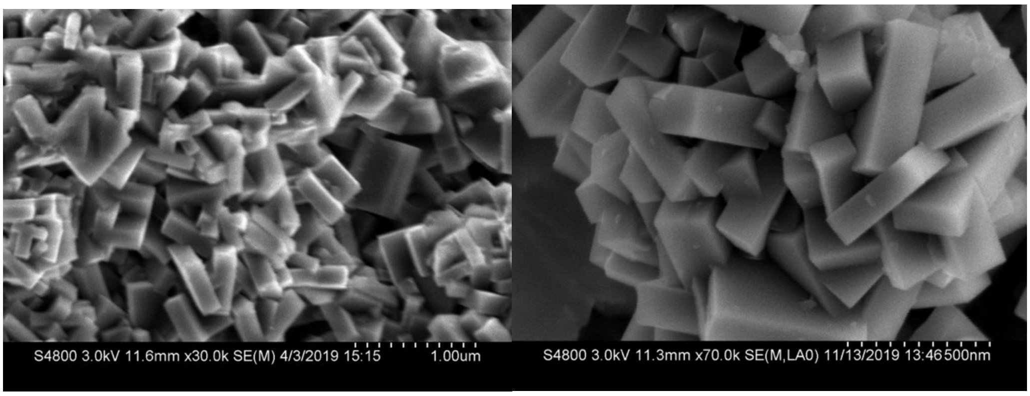

Figure S12. SEM images of the samples at all time points (14%).

SC1. Sodium binding energy calculations

DFT calculations were performed to optimize the geometries of OSDA molecules in SSZ-39 with exclusively cis isomers, exclusively trans isomers and a 50:50 mixture of cis and trans OSDA isomers in the SSZ-39 framework with one OSDA per SSZ-39 cage. 26 Aluminum pair calculations were tested for SSZ-39 with each aluminum pair testing 3 initial starting orientations for each OSDA combination. The details of these OSDA calculations are discussed in Section SC 2.2. Similar calculations were performed with FAU with exclusively cis and exclusively trans OSDA molecules present. Once the orientations of the OSDA molecules had been determined and the most favorable aluminum pair distributions had been determined we then proceeded to calculate the binding energies of sodium by determining the energy associated with reacting a Brønsted acid site with NaOH to form water and replace the Brønsted acid site with a sodium atom bound to the zeolite using the equation below.

$$E_b = ZNa - ZH - NaOH + H_2O(g)$$

Where E_b is the binding energy ZH is the energy of the zeolite with two Al atoms charge comepensated by an OSDA molecule and the third charge compensated by a Brønsted acid site, and ZNa is the energy of the zeolite with with two Al atoms charge comepensated by an OSDA molecule and the third charge compensated by a sodium atom. Finally, $H_2O(g)$ is a water molecule in the gas phase.

The binding energy of sodium was calculated for the most favorable structure for each OSDA pair in SSZ-39 and each OSDA in FAU. The binding energy of sodium was calculated so as to charge compensate a new aluminum atom in each T site capable of holding an aluminum atom without violating Löwenstein's rule. For each T site 4 initial adsorption positions were tested with each position being anti to one of the adjacent oxygen sites. Once initial binding energy calculations had been performed, we found that a double six membered ring site containing 2 aluminum atoms (refered to as a 2Al-D6MR site) to be the best adsorption position for sodium with exclusively cis and exclusively trans OSDA isomers. This site was not sampled in the 50:50 cis trans configuration since both OSDAs charge compensate an aluminum atom in this 2Al-D6MR site. To determine if this site was also the most favorable position in a 50:50 isomer mixture, binding energy calculations were repeated where the sodium atom had been moved to the 2Al-D6MR site and one OSDA had been reoriented to charge compensate the aluminum atom previously charge compensated by sodium. This process was repeated to test four orientations for each OSDA.

SC2. OSDA siting details for multiple OSDAs in SSZ-39

SC 2.1 Aluminum Distribution Generation

To generate SSZ-39 frameworks we acquired the SSZ-39 framework structure from the international zeolite association database of zeolite frameworks [1]. We then converted the atomic coordinates to the Niggli reduced cell using the Visualization for Electronic and Structural Analysis (VESTA) software [2]. We then used the Multiscale Atomistic Zeotype Simulation Environment software package [3] to generate all unique aluminum pair distributions in our unit cell that obey Löwensteins rule.

SC 2.2 Initial OSDA position generation

When calculating the binding energies of organic structure directing agents in zeolites, changes in the initial orientation of the OSDA molecule can lead to significant shifts in the final geometries and energies calculated by DFT programs due to the inability of most optimization algorithms to distinguish between local and global minimums. When only a single OSDA molecule is present in the zeolite framework it is feasible to simply calculate each potential initial orientation, however when multiple OSDAs are present in the framework the number of calculations necessary to exhaustively test each initial orientation quickly grows too large to be realistic. In order to limit the influence of local minimums on our results we used the following procedure to generate and screen initial OSDA positions. Initial positions were generated with each of the following three methods, placing charge compensating species in Materials Studio [4] with positions and orientations based on experimental observations, generating initial positions using LEGO [5-7] and screening using either single point VASP calculations or LAMMPS geometry optimizations. In cases where configurations were screened using VASP single point calculations 100 initial positions were considered, in cases where LAMMPS was used to screen OSDA orientations 1000 initial positions were considered. In both cases the most favorable structure was then evaluated using VASP. A diagram of the workflow can be seen in Figure S13.

SC 2.2 Force Field Calculation Details

All force field calculations were performed using the Large-scale Atomic/Molecular Massively Parallel Simulator (LAMMPS) software package [8]. We used the Deriding force field to model atoms permanently bonded together which has been shown to be effective at modeling zeolite-OSDA systems. In our models the atoms in the zeolite framework were fixed in place and the OSDA molecules were rigid. In order to examine the effectiveness of our force field models in accurately calculating the energetics of zeolite OSDA pairings we randomly selected a zeolite OSDA pair and used VASP to calculate the energy of the optimized configurations for each of the 1000 configurations screened by LAMMPS and compared the relative energies (Figure S14). The results indicated a strong correlation between energies calculated by LAMMPS and energies calculated by VASP, giving us confidence LAMMPS could be used to identify promising initial configurations

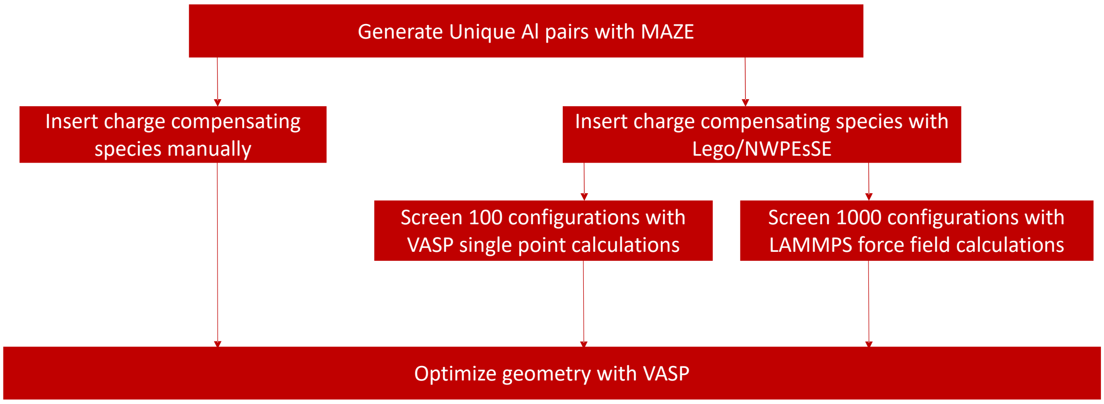

Figure S13. Workflow for OSDA siting in SSZ-39.

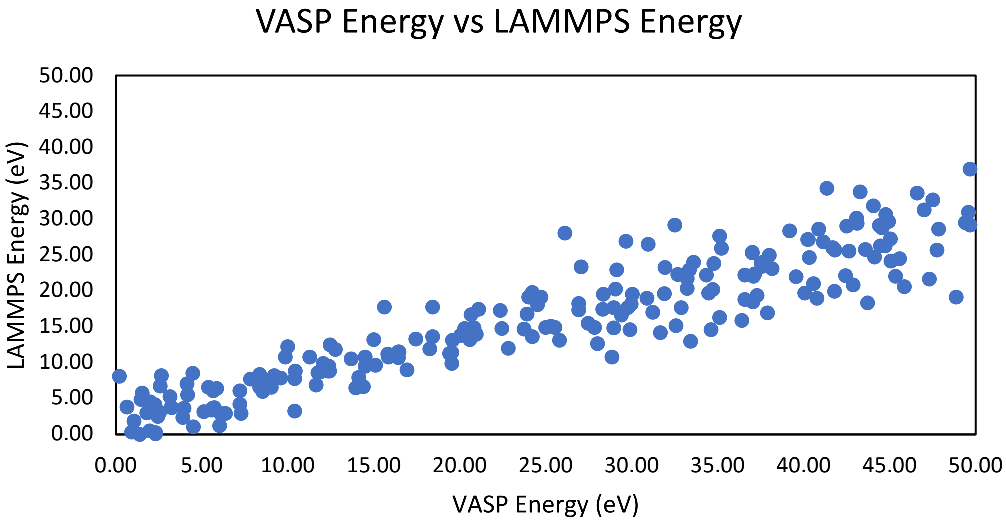

Figure S14. Energies calculated by VASP compared to energies calculated by LAMMPS for the ground state energies of OSDA isomers in SSZ-39.

System	Final Geometries	Sodium Binding Energy (kJ/mol)
FAU-Trans	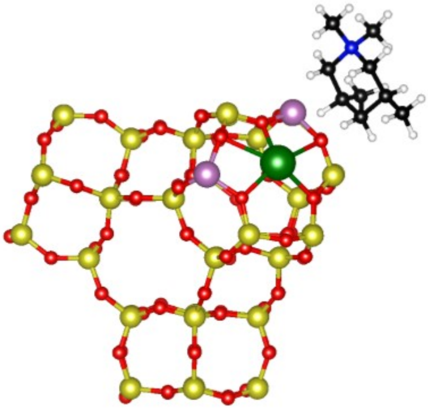	-301.1

FAU-Cis	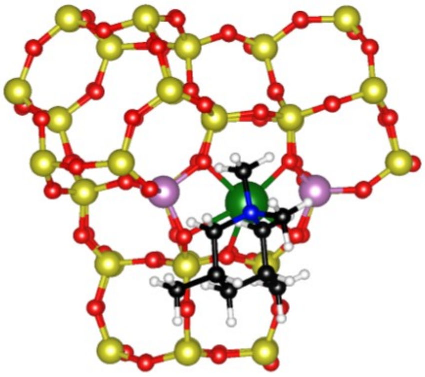	-302.9
SSZ-39-Cis	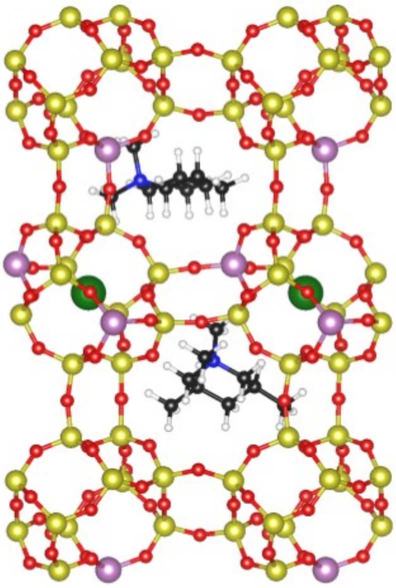	-315.9

SSZ-39-Cis/Trans Ideal sodium position	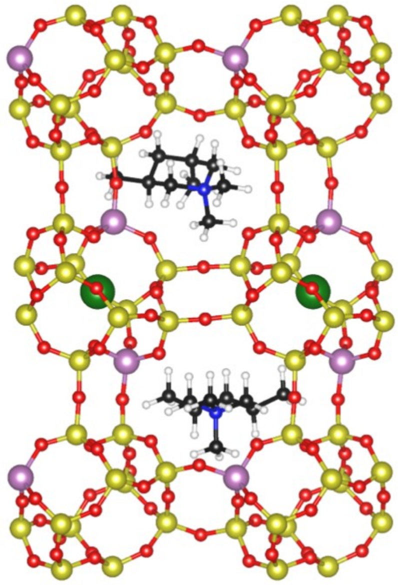	-304.5
SSZ-39-Cis/Trans Ideal OSDA orientation position	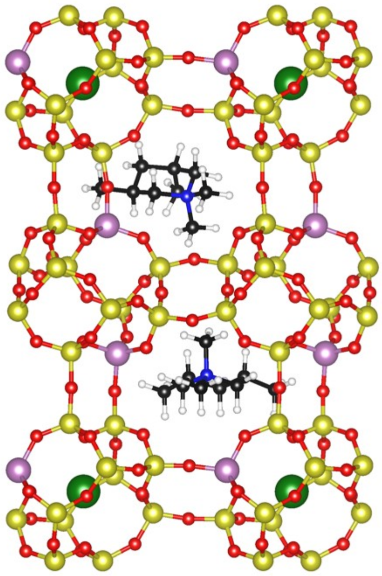	-292.7

SSZ-39-Trans	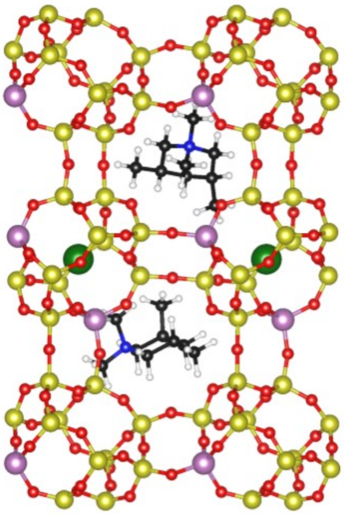	-315.5

Table S1. Most favorable sodium absorption positions in FAU and SSZ-39 with different OSDA isomers co-absorbed. The red, yellow, cyan, black, blue and white spheres are O, Si, Al, C, N and H atoms, respectively.

System	OSDA in Ideal Orientation	Sodium in Ideal Position
Geometry		
Binding Energy (kJ/mol)	-292.7	-304.5

Table S2. SSZ-39 with sodium bound in a 50-50 cis-trans mixture with the OSDAs in their ideal position and with the cis OSDA reoriented to enable the sodium atom to sit in the more favorable 2Al-D6MR position. The color coding is the same as in Table S1.

SC 2.3 Rotation Energy Calculations.

To determine the energy penalty associated with reorienting the cis OSDA in the SSZ-39 structure the structures in Table S2 were altered by removing the sodium and the replacing the aluminum atom formerly charge compensated by sodium with a silicon atom. The resulting figures can be seen in **Table S3.** Single point calculations were then performed on these structures with the rotation energy penalty defined as the difference in energy between the structure with OSDA molecules in their ideal configuration and the structure with the cis OSDA rotated.

$$E_{rotation} = E_{ideal\ OSDA\ orientation} - E_{rotated\ OSDA}$$

System	Ideal OSDA Positions	Rotated OSDA
Geometry	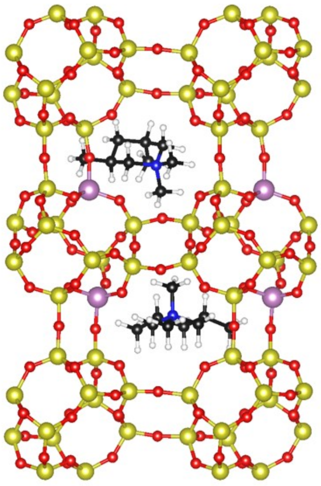	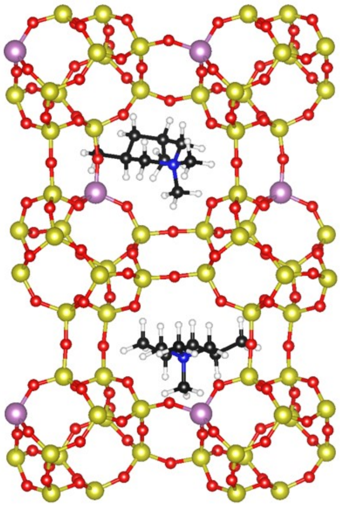

Table S3. Configurations used to determine rotation energy penalty. The rotated OSDA configuration results in an energy that is 2.15 kJ/mol less favorable than the ideal OSDA orientation configuration. The color coding is the same as in Table S1.

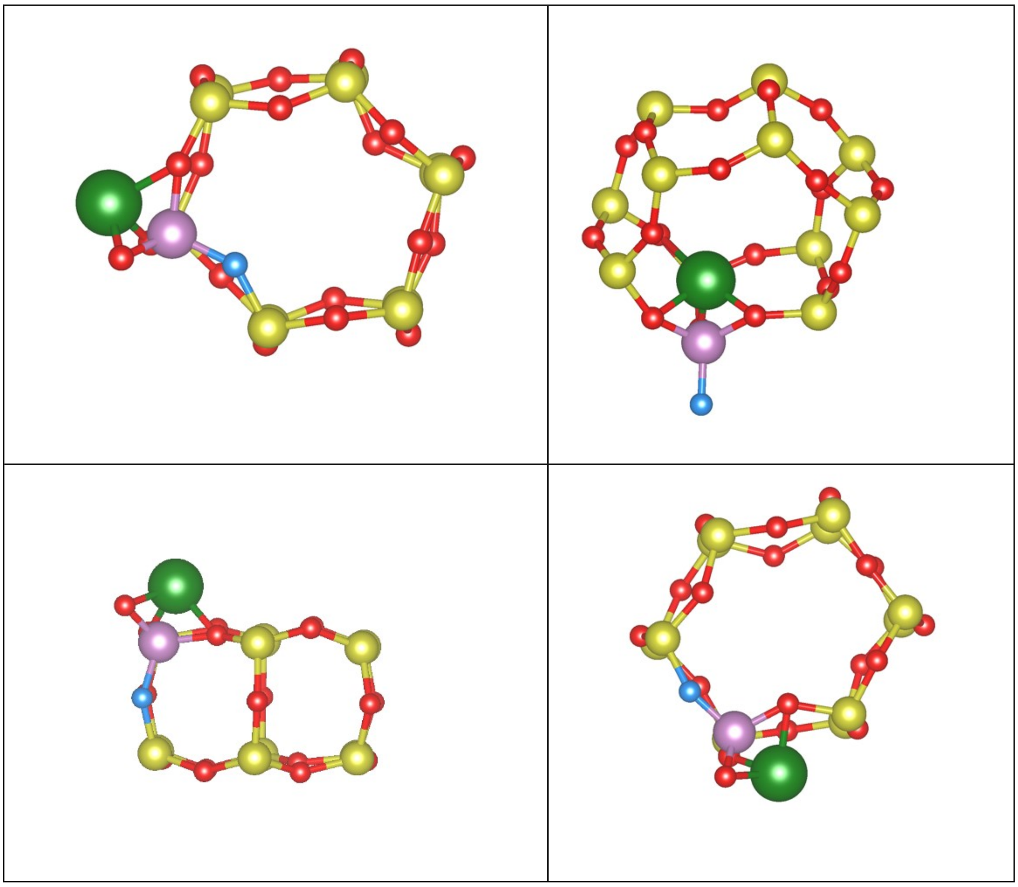

Figure S12. Example of initial sodium placement for an Al site. A configuration is made containing sodium placed anti to an oxygen bounded to the adjacent aluminum atom. In the figure above the anti oxygen is colored blue. Geometry optimizations are then preformed to find the nearest local minimum for each initial position with the most favorable local minimum being used to determine the sodium binding energy. The color coding of the other spheres is the same as in Table S1.

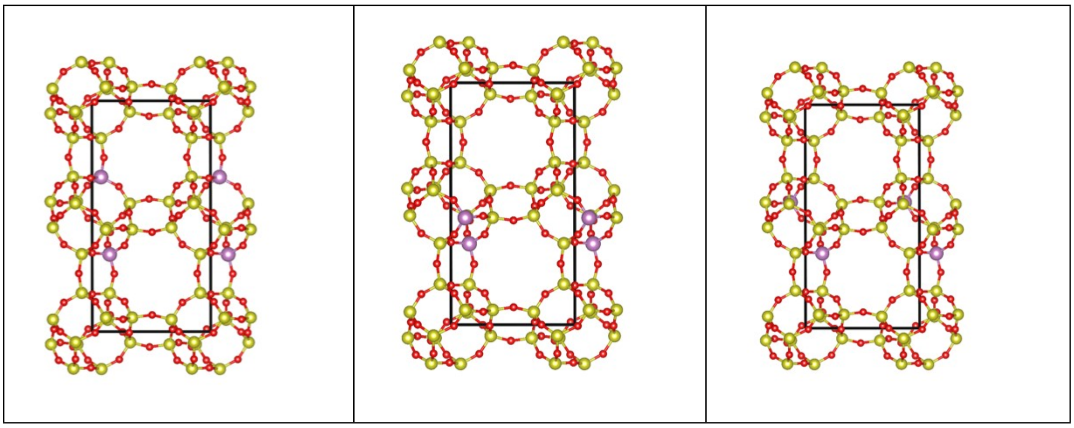

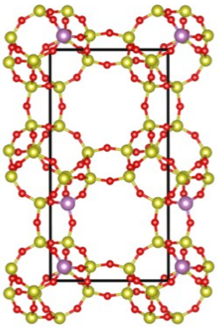

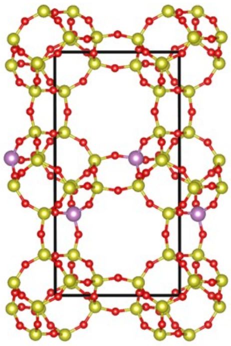

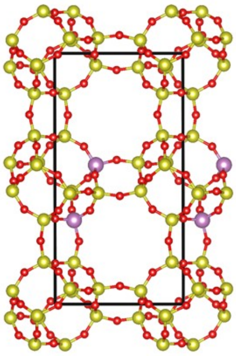

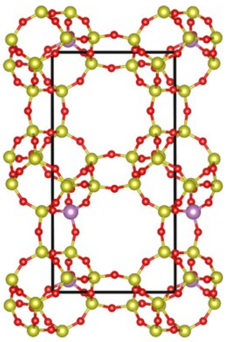

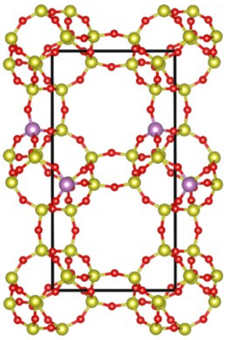

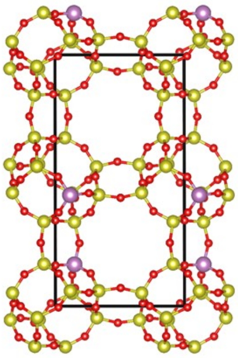

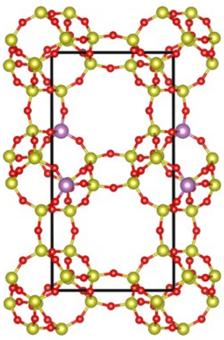

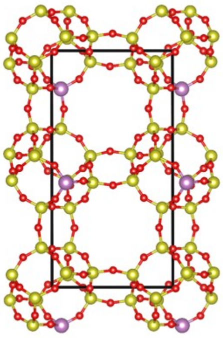

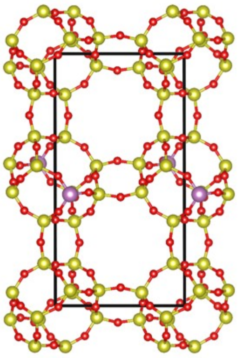

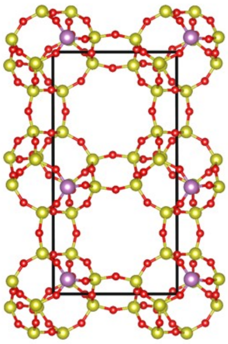

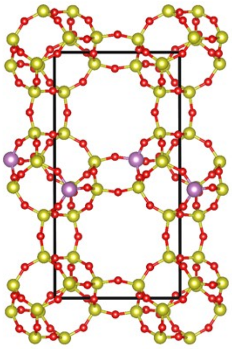

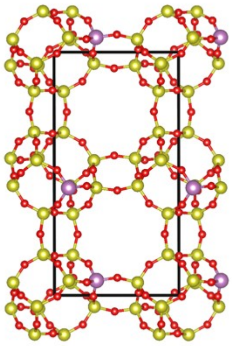

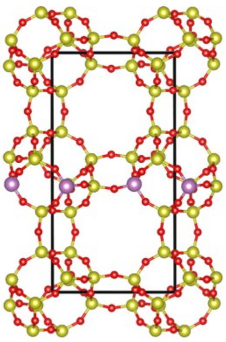	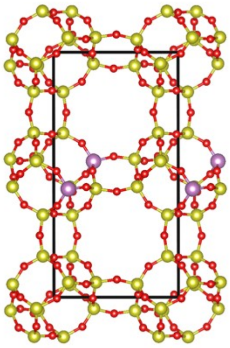	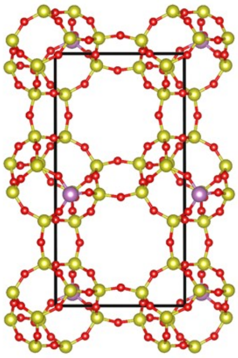
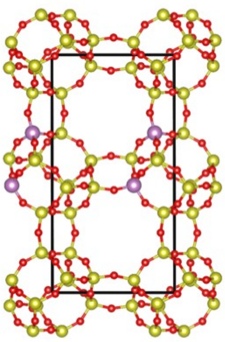	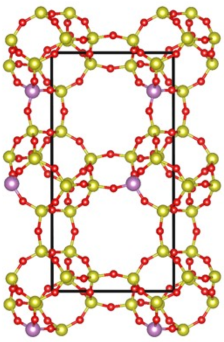	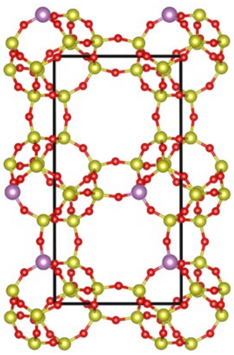
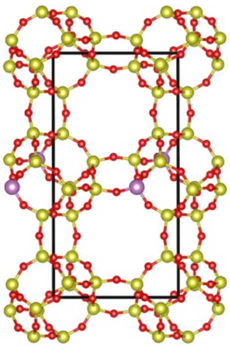	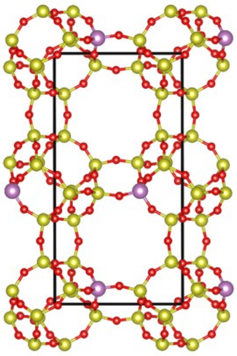	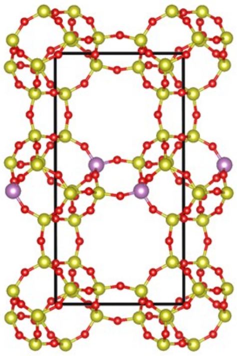
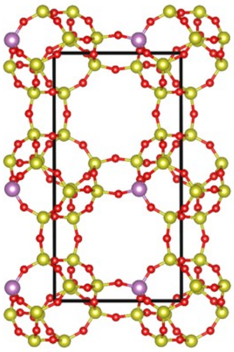	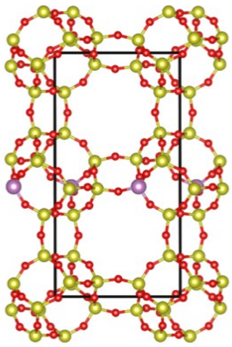	

Table S4. Aluminum distributions considered for aluminum pair calculations with the computational unit cell included. The color coding is the same as in Table S1.

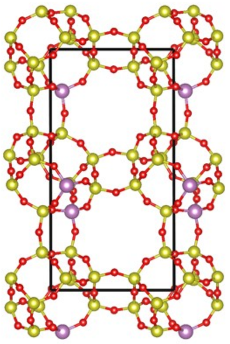	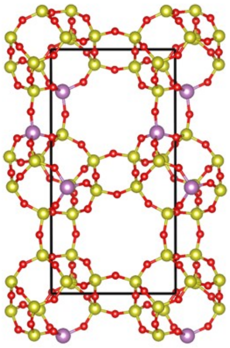	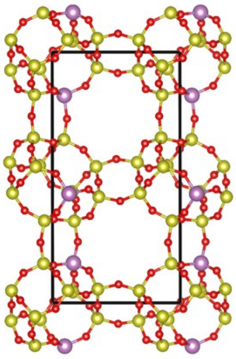
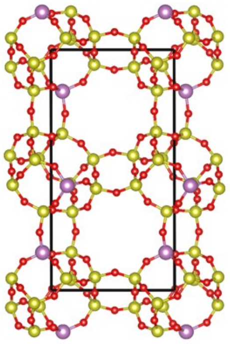	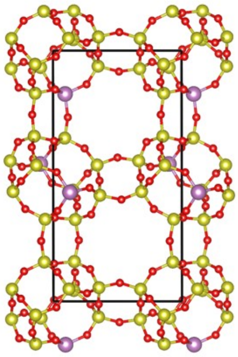	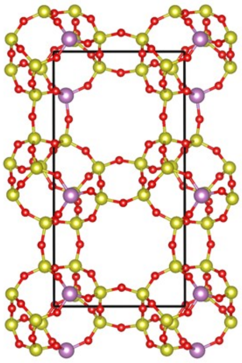
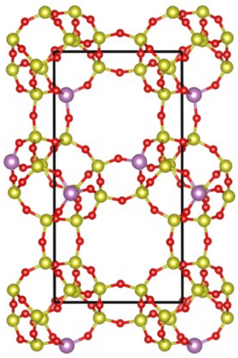	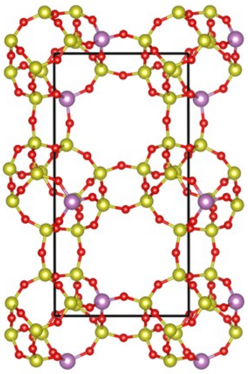	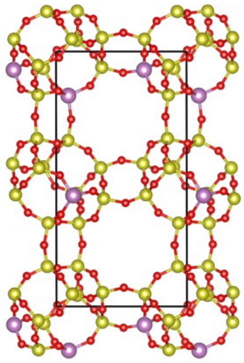
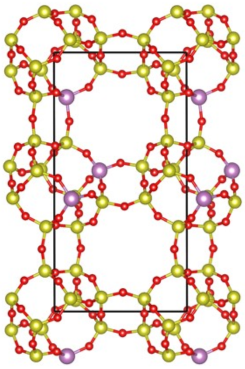	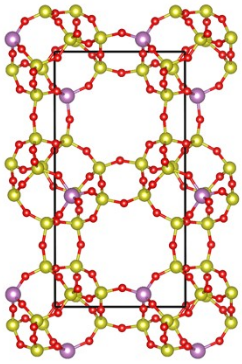	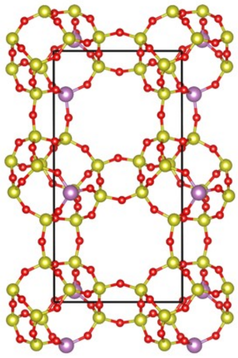

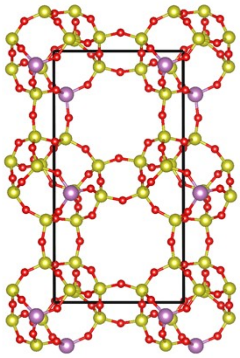		

Table S5. Aluminum distributions considered for sodium binding energy calculations with exclusively cis OSDA molecules. The color coding is the same as in Table S1.

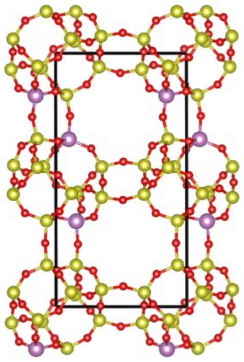	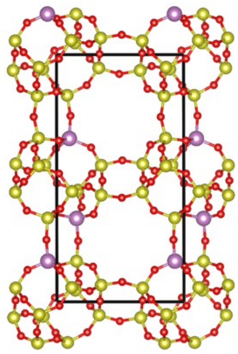	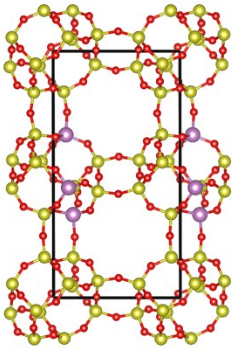
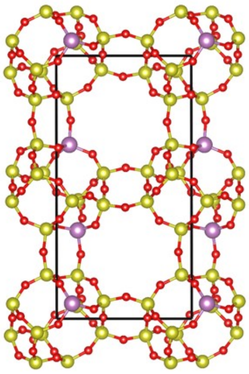	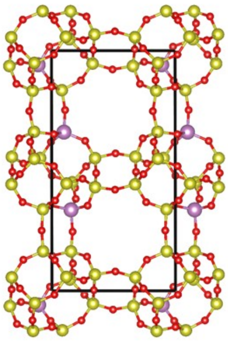	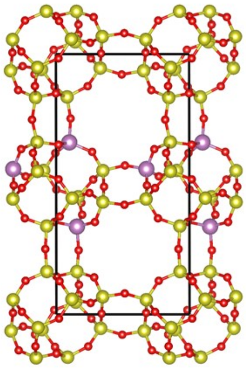
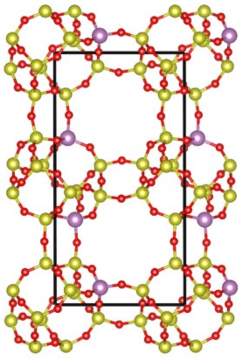	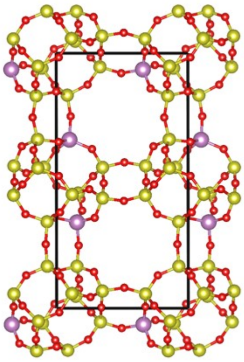	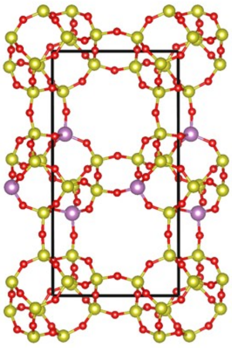

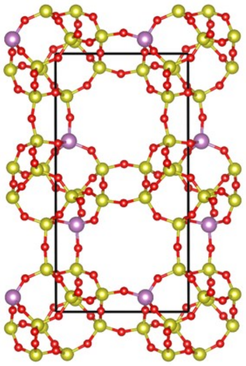	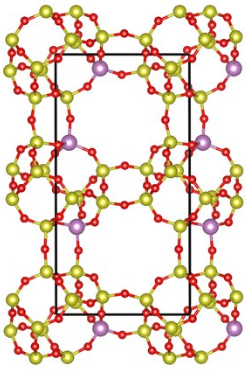	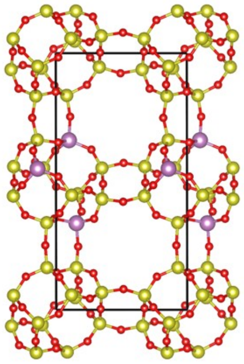
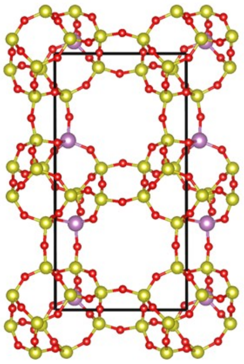	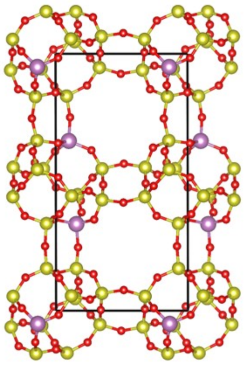	

Table S6. Aluminum distributions considered for sodium binding energy calculations with a mixture of cis and trans OSDA molecules. The color coding is the same as in Table S1.

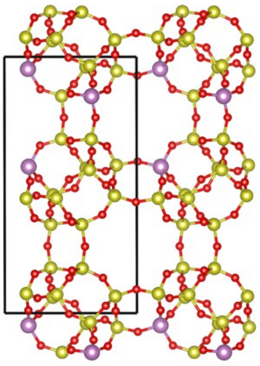	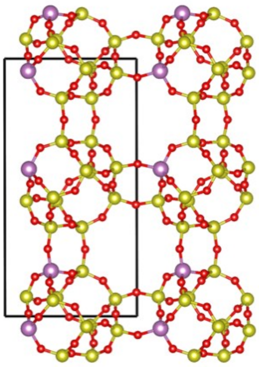	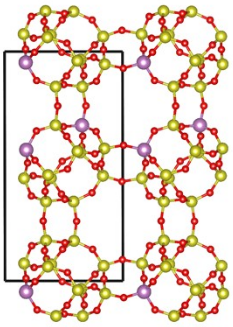
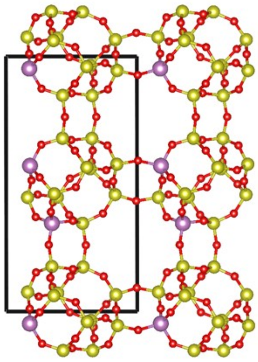	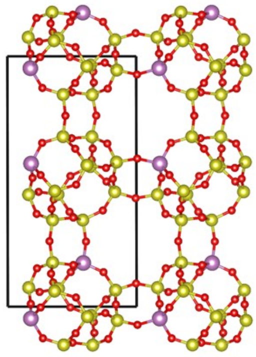	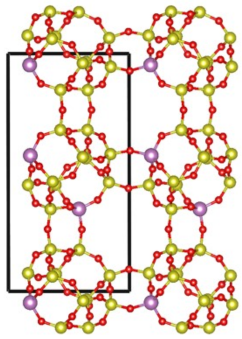

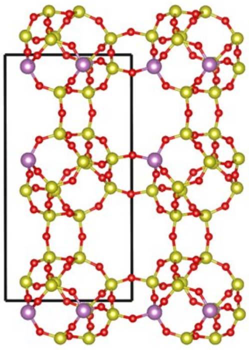	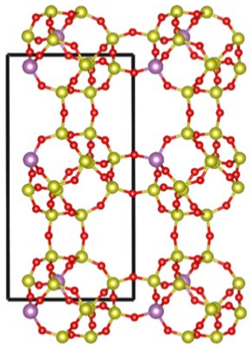	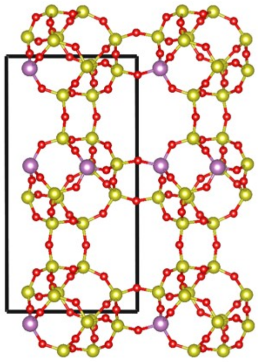
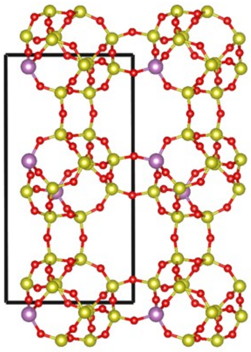	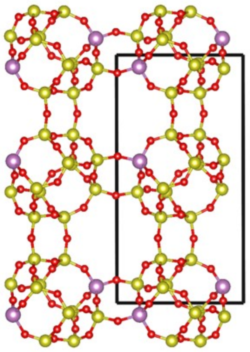	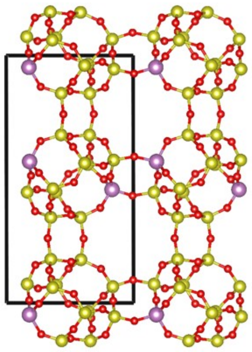
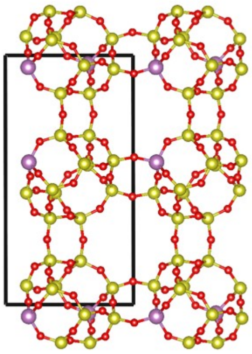	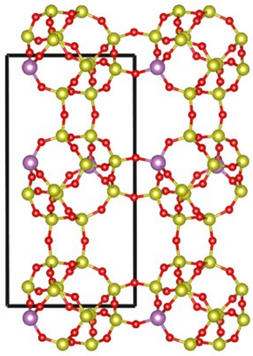	

Table S7. Aluminum distributions considered for sodium binding energy calculations with exclusively trans OSDA molecules. The color coding is the same as in Table S1.

Reaction time	4 h	8 h	12 h	18 h	24 h	72 h
Trans%	Si/Al					
14%trans	4.7	5.3	7.1	6.8	7.6	7.7
26%trans	4.7	5.8	7.1	7.3	7.8	7.9
54%trans	4.8	6.1	7.3	7.5	8.0	8.0
80%trans	4.7	6.5	7.4	8.5	8.6	8.6

Table S8. Composition of solids obtained from the synthesis work as a function of heating time.

References

1. C. Baerlocher and L. B. McCusker, *Database of Zeolite Structures*.
2. K. M. a. F. Izumi, *J. Appl. Crystallogr.*, 2011, **44**, 1272-1276.
3. D. D. Antonio, J. Guo, S. J. Holton and A. R. Kulkarni, *SoftwareX*, 2021, **16**.
4. BIOVIA, Dassault Systèmes, BIOVIA Materials Studio).
5. J. Zhang and M. Dolg, *Phys. Chem. Chem. Phys.*, 2015, **17**, 24173–24181.
6. J. Zhang and M. Dolg, *Phys. Chem. Chem. Phys.*, 2016, **18**, 3003-3010.
7. J. Zhang, Glezakou, V.-A., Rousseau, R. & Nguyen, M.-T., *J. Chem. Theory Comput.*, 2020, **16**, 3947-3958.
8. A. P. Thompson, H. M. Aktulga, R. Berger, D. S. Bolintineanu, W. M. Brown, P. S. Crozier, P. J. in't Veld , A. Kohlmeyer, S. G. Moore, T. D. Nguyen, R. Shan, M. J. Stevens, J. Tranchida, C. Trott and S. J. Plimpton, *Comput. Phys. Commun.*, 2022, **271**, 108171.